

Towards Efficient Dye-Sensitized Solar Cells: An economical Strategy for Prototypical Organic Dyes with Tailored Frontier Orbitals

Aditi Singh,^{1,*} Ram Dhari Pandey,^{1,†} Subrata Jana,¹ Prasanjit Samal,² Paweł Tecmer,¹ and Szymon Śmiga^{1,‡}

¹ Institute of Physics, Faculty of Physics, Astronomy and Informatics,
Nicolaus Copernicus University in Toruń, ul. Grudziądzka 5, 87-100 Toruń, Poland

² School of Physical Sciences, National Institute of Science Education and Research,
An OCC of Homi Bhabha National Institute, Bhubaneswar 752050, India

(Dated: January 15, 2026)

The computational design of heteroatom-doped organic dyes remains challenging, requiring methods that are accurate for charge transfer (CT) properties yet efficient enough to explore large chemical spaces. Here we enable rapid and reliable screening using the range-separated hybrid functional LC- ω PBE ground state and linear-response Time Dependent Density Functional Theory, combined with a recently proposed simplified and physically motivated effective tuning protocol (ω_{eff}).

Using this approach we have investigated CT excitations energies and frontier orbital alignment, which are central to designing dye-sensitized solar cells (DSSCs) - through the strategic incorporation of heteroatoms (N, O, B) into a series of D- π -A dyes. A library of 27 mono-, di-, and tri-doped organic dyes derived from a carbazole donor and cyanoacrylic acid acceptor is constructed by targeted doping at three critical sites of the bridge. The library reveals clear, tunable design rules: electron-rich N and O dopants systematically increase the HOMO-LUMO gap and excitation energies (with N inducing a stronger blue shift than O), while electron-deficient B incorporation reduces gaps and produces pronounced red shifts. The BBN-doped variant emerges with the smallest gap and lowest excitation energies. Overall, this work provides a curated dataset, practical doping guidelines, and, critically, a computationally efficient and reliable tuned-DFT protocol for the accelerated discovery of optimized organic dye sensitizers.

INTRODUCTION

Charge transfer (CT) phenomena are crucial in the fields of physics, chemistry, and biology, occurring across both natural and synthetic systems. These phenomena are observed in diverse contexts, including organic semiconductors, [13, 59] Deoxyribonucleic acids (DNAs) [63, 79], photocatalytic processes, [37] and enzyme related reactions. [47] The importance of CT is exemplified by several key processes e.g.: it enables photosynthetic electron shuttling in chlorophyll reaction centers (e.g., PSII) for solar energy conversion[92], catalytic water splitting in molecular assemblies (e.g., $[\text{Ru}(\text{bpy})_3]^{2+}/\text{TiO}_2$) for renewable H_2 production[39] or redox-driven fluorescence switching in DNA-based biosensors for real-time pathogen detection. Furthermore, CT dynamics govern exciton dissociation and carrier transport in organic solar cells (OSCs), where donor-acceptor heterojunctions (e.g., PM6:Y6) achieve around 15% power conversion efficiencies by optimizing the charge. Among various factors that impact CT phenomena in organic dyes, the energy levels, specifically the highest occupied molecular orbital (HOMO) and lowest unoccupied molecular orbital (LUMO) of a sensitizer, are crucial for designing dye-sensitized solar cells (DSSC). These orbitals provide critical information about the efficiency of CT. To design artificial sensitizers mainly two types of molecules are used. First, we have Ruthenium-based complexes, [80] which are expensive because of the complicated purification process. In contrast, metal-free organic dyes offer many advantages, including a large absorption coefficient, [29]

simple and low-cost synthesis process, [2, 20, 54] an environmental friendly approach, and a broad photon spectrum that facilitates efficient charge separation across the dye molecule [46]. A wide range of metal-free organic dyes have been studied with different configurations such as D-A- π -A [4, 96], D-D- π -A [49], D- π -A [97], D- π -A-A [67], where D and A are donor and acceptor, respectively. Among them, the widely accepted and highly promising approach for molecular design of efficient metal-free organic sensitizers is the donor- π -bridge-acceptor (D- π -A) model [35, 36, 53], which allows intramolecular CT. In this framework, the possibility of optimal donor units such as triphenylamine, [86, 94] coumarin, [23, 70, 91] carbazole, [18, 38] and phenothiazine being the best option due to their strong electron-donating capacity. The π -conjugated bridge, often composed of different moieties such as perylene, [8, 25] enediyne, [90] thiophene and fused benzene rings, serves as a crucial linker between the donor and acceptor. Finally, cyanoacrylic acid is the predominant acceptor and anchoring group, [68, 73, 98] as it effectively withdraws electrons from the donor via its cyano group (-CN) while its carboxylic acid group (-COOH) binds to the TiO_2 surface. When photons are absorbed by an organic dye, electrons are excited from the HOMO to the LUMO. [1] To achieve efficient device operation, two key energy level conditions must be met. [29] First, the HOMO level of the dye must be significantly below the redox potential ($-4.80 \text{ eV } I^-/I_3^-$) of the electrolyte for efficient regeneration of the dye. Second, the LUMO energy level of the organic dye should be above the energy level of the con-

duction band (-4.0 eV TiO_2) of the semiconductor. This alignment facilitates the injection of photoexcited electrons from the dye's LUMO into the conduction band. Based on our review of the current literature, and to the best of our knowledge, there remains a substantial gap in understanding the electronic structures of carbazole-based systems featuring five-membered, heteroatom-doped π -bridges. [16, 85]

Only a few systems have been studied, leaving this area largely unexplored so far. The limited exploration is primarily caused by several challenges contributing to this difficulty i.e. (i) the complexity and computational cost of the systems, especially with wave function theory (WFT) methods[17, 33, 43, 84]; (ii) the constraints of using small basis sets[17, 34, 58, 71] which in context of WFT methods can provide no so reliable predictions[14]; (iii) the lack of cost-effective approaches that can efficiently and accurately explore the broad chemical space of possible complexes while maintaining predictive accuracy[15–17, 56–58, 71]. As a result, the lack of organized datasets and systematic studies have prevented a clear understanding of how doping affects DSSC properties.

To efficiently sweep a broad chemical space of possible DSSC complexes, our computational workflow combines ground-state Kohn-Sham density functional theory (KS-DFT) and linear-response time-dependent DFT (TDDFT) for excited-state properties treatment. The former calculations have been performed using the range-separated hybrid (RSH) functional LC- ω PBE [89], which is well suited for describing CT character due to its correct long-range treatment of exchange energy[52, 76, 81] and potential[45]. In turn, the range-separation (RS) parameter ω was set using the recently proposed efficient ω_{eff} tuning protocol [76], which has been shown to provide near-IP-tuning accuracy at a substantially reduced computational cost. This methodology provides a physically motivated, system-dependent starting point that has been empirically validated for CT state prediction[76]. Moreover, recent studies have demonstrated that ω_{eff} serves as an excellent starting point for single-shot Green's function approximation G_0W_0 calculations within many-body perturbation theory[77]. This dual validation within both TDDFT and G_0W_0 frameworks substantiates the robustness of ω_{eff} as a reliable parameter for both predicting properties of existing CT systems and guiding the design of novel donor-acceptor architectures.

By leveraging these methods to address the existing gap in the literature and enable rational materials design, we systematically investigate mono-, di-, and tri-doped organic dyes consisting of a common carbazole donor and a cyanoacrylic acid acceptor.

The paper is organized as follows. Section 2 provides the methodological background, and Section 3 presents and discusses the results. Finally, Section 4 provides con-

cluding remarks and future perspectives.

METHODOLOGY

Methods

Within this study, ground-state electronic structure properties were obtained using the LC- ω PBE RSH density functional approximation (DFA) [89]. This functional decomposes the exchange interaction into short-range (SR) and long-range (LR) components via the error function formalism [95]

$$\frac{1}{r} = \frac{\alpha + \beta \operatorname{erf}(\omega r)}{r} + \frac{1 - [\alpha + \beta \operatorname{erf}(\omega r)]}{r}, \quad (1)$$

where the LC- ω PBE takes the form

$$E_{xc}(\omega) = E_x^{\text{LR},\text{HF}}(\omega) + E_x^{\text{SR},\text{PBE}}(\omega) + E_c^{\text{PBE}}, \quad (2)$$

with $\alpha = 0$ and $\beta = 1$, $E_x^{\text{LR},\text{HF}}(\omega)$ is the LR Hartree-Fock (HF) exchange, $E_x^{\text{SR},\text{PBE}}(\omega)$ is the SR PBE exchange functional and ω is the range separated parameter. Finally, E_c^{PBE} denotes the standard PBE correlation functional without range separation.

The LC- ω PBE has proven especially reliable for modeling CT excitations [52, 76, 81]. The performance stems from its formal construction: it enforces 100% exact HF exchange in the long-range limit ($r \rightarrow \infty$). As a result, the exchange potential exhibits the correct $-1/r$ asymptotic decay, which is crucial for accurately describing the spatial separation between electron donors and acceptors in CT processes.

For the range-separation parameter ω , we have utilize the effective tuning scheme which provides a physically motivated, system-dependent starting point that has been empirically validated for CT state prediction[76, 77]. In this case the ω parameter is determined as

$$\omega_{eff} = \frac{a_1}{\langle r_s \rangle} + \frac{a_2 \langle r_s \rangle}{1 + a_3 \langle r_s \rangle^2} \quad (3)$$

where $a_1 = 1.91718$, $a_2 = -0.02817$, and $a_3 = 0.14954$, with average Wigner-Seitz radius $\langle r_s \rangle$ computed as

$$\langle r_s \rangle = \frac{\int \operatorname{erf} \left(\frac{\rho(\mathbf{r})}{\rho_c} \right) r_s(\mathbf{r}) d^3r}{\int \operatorname{erf} \left(\frac{\rho(\mathbf{r})}{\rho_c} \right) d^3r}. \quad (4)$$

The $\rho_c = \rho_{\text{th}} / \int \rho(\mathbf{r}) d^3r$, in turn, defines the density cut-off threshold, which is a system-dependent quantity. For the full derivation, physical interpretation, and parameterization of this effective form, we refer the reader to Ref. 76.

The theoretical framework of linear-response TDDFT computes excitation energies via the solution of a non-Hermitian eigenvalue problem[10, 11, 26]

$$\begin{pmatrix} \mathbf{A} & \mathbf{B} \\ \mathbf{B}^* & \mathbf{A}^* \end{pmatrix} \begin{pmatrix} \mathbf{X} \\ \mathbf{Y} \end{pmatrix} = \omega \begin{pmatrix} \mathbf{1} & \mathbf{0} \\ \mathbf{0} & -\mathbf{1} \end{pmatrix} \begin{pmatrix} \mathbf{X} \\ \mathbf{Y} \end{pmatrix}, \quad (5)$$

where ω is the excitation energy. The matrices \mathbf{A} and \mathbf{B} are defined by

$$A_{ia,jb} = \delta_{ij}\delta_{ab}(\epsilon_a - \epsilon_i) + (ia|jb) + (ia|f_{xc}(r, r')|jb), \quad (6)$$

$$B_{ia,jb} = (ia|bj) + (ia|f_{xc}(r, r')|bj) \quad (7)$$

where ϵ_i and ϵ_a are the KS orbital energies of the occupied and virtual states, respectively. The term $(ia|jb)$ represents the two-electron repulsion integral, defined as $(ia|jb) = \iint d\mathbf{r} d\mathbf{r}' \psi_i^*(\mathbf{r}) \psi_a(\mathbf{r}) \frac{1}{|\mathbf{r} - \mathbf{r}'|} \psi_j^*(\mathbf{r}') \psi_b(\mathbf{r}')$. The exchange-correlation kernel is given by $f_{xc}(\mathbf{r}, \mathbf{r}') = \frac{\delta^2 E_{xc}[\rho]}{\delta \rho(\mathbf{r}) \delta \rho(\mathbf{r}')}\Big|_{\rho_0}$, evaluated at the ground-state electron density ρ_0 .

The eigenvectors \mathbf{X} and \mathbf{Y} represent the transition amplitudes, where the \mathbf{X} vector corresponds to the particle-hole (excitation) channel, while the \mathbf{Y} vector corresponds to the hole-particle (de-excitation) channel. The presence of the \mathbf{B} matrix couples these channels, leading to the non-Hermitian structure of the eigenvalue problem.

To ensure computational efficiency while maintaining accuracy, in our study we have adopted the Tamm-Danoff approximation (TDA). Within this approximation the off diagonal \mathbf{B} matrix elements are set to zero[32] leading to simplified Hermitian eigenvalue problem

$$\mathbf{AX} = \omega^{\text{TDA}} \mathbf{X} \quad (8)$$

Equation (8) has few practical advantages i.e. (i) as it is a standard Hermitian eigenvalue problem, for which highly efficient and robust numerical solvers exist[61, 82]. (ii) it avoids the occurrence of spurious low-lying excitations that can sometimes appear in the full TDDFT treatment of charge-transfer states or systems with a small fundamental gap[51, 64, 72]. (iii) it often provides a very good description of excited states that are dominated by single excitations[9, 32]. While TDA neglects the coupling to de-excitations, which can be important for a rigorous description of oscillator strengths and some double excitations, it has proven to be a highly accurate and efficient workhorse for computing excitation energies in molecular systems[72].

Computational details

The geometric structures for a series of mono-, di-, and tri-doped organic dyes were optimized in a vacuum using KS-DFT with the BP86 [6, 60] functional

and the cc-pVDZ basis set, [19] using ORCA software package [55]. All optimized structures were confirmed as true energy minima by the absence of imaginary frequencies in subsequent vibrational frequency analysis. The corresponding xyz coordinates for all structures are available in Ref. [74]

Electronic structure calculations were conducted within the framework of KS-DFT using the long-range-corrected LC- ω PBE functional in combination with the Def2-TZVPD basis set for all molecular systems. This approach enabled the accurate determination of frontier molecular orbital energies, including the HOMO and LUMO orbitals, as well as the corresponding HOMO-LUMO energy gaps. Excited-state properties were subsequently computed using TDA to obtain vertical excitation energies. All electronic structure calculations were carried out using the Q-Chem[22] software package. The resulting frontier molecular orbitals were visualized and analyzed using the Jmol software package[30] to examine orbital distributions, and spatial localization features relevant to CT processes.

The ω_{eff} parameter have been computed using PySCF [83] with a publicly available tuning protocol[75]. This protocol employs an averaging approach that exhibits minimal sensitivity to variations in functional or basis set selection.[76] Moreover, for comparison we have also determined the optimal ω parameter using IP-tuning procedure as

$$\omega_{IP} = \arg \min_{\omega} |\text{IP}(\omega) + \epsilon_{\text{HOMO}}(\omega)|. \quad (9)$$

Although this tuning procedure may fail in some cases for CT systems[5] the comparison with effective tuning is important to validate the whole computational protocol. In this case the range-separation parameter ω is optimized to satisfy the ionization potential (Koopmans' theorem) condition[44, 65]. This step is done in order to systematically compare the robustest of effective tuning. The IP-tuned parameter is determined via Q-Chem software[22], with aug-cc-pVDZ[40] basis and LC- ω PBE functional for optimization. This basis has been used for multiple investigations Ref[44, 66, 88], and points towards passive impact with a larger basis.

Doped systems

We constructed a comprehensive library of doped organic dyes by selectively replacing carbon atoms with heteroatoms (**N**, **O**, **B**) at three critical linker sites (denoted as positions *a*, *b*, and *c*). The library was systematically designed to include mono-, di-, and tri-doped configurations. For mono-doping, we designed three isomers for both nitrogen (**NCC**, **CNC**, **CCN**) and oxygen (**OCC**, **COC**, **CCO**) and two isomers for boron (**BCC** and **CBC**), yielding a total of eight mono-doped systems. Di-doping yielded both homogeneous (**NNC**, **CNN**, **NCN**,

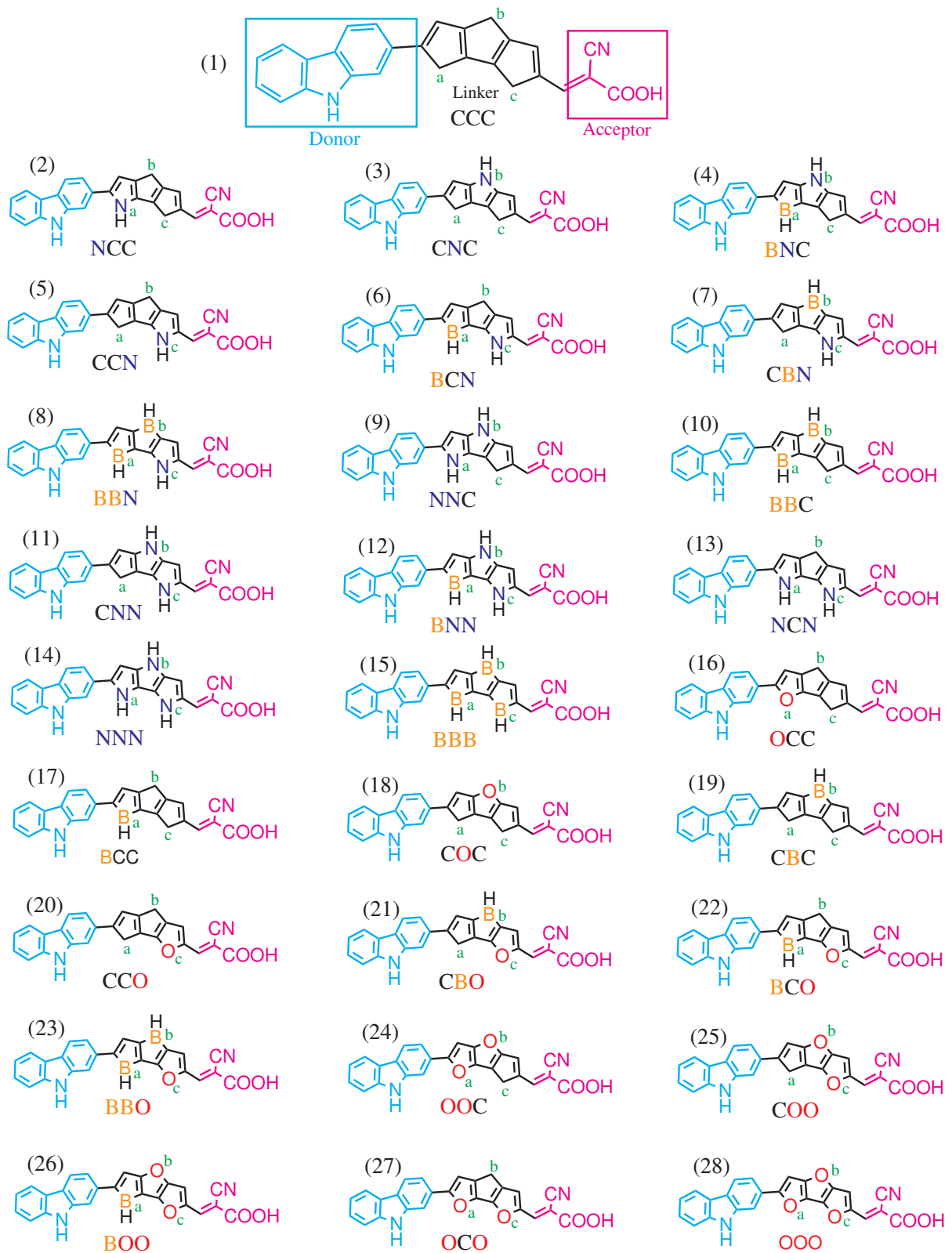


FIG. 1. Schematic representation of a library that consists of a series of 27 mono-, di-, and tri-doped prototypical organic dyes with common donor and acceptor moieties.

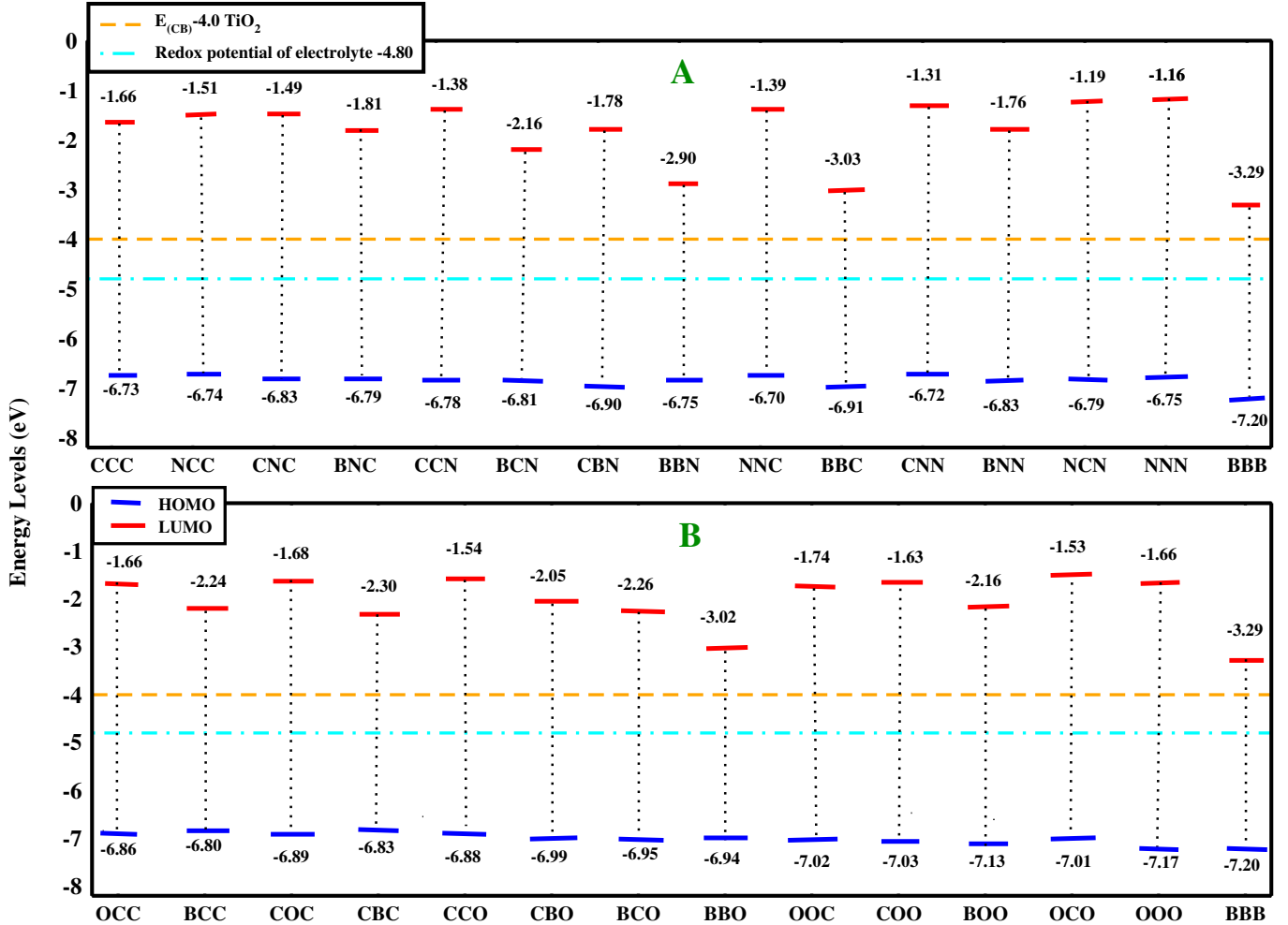


FIG. 2. The HOMO and LUMO energy levels (eV) of N- and B-doped (A) and O- and B-doped (B) organic dyes, analyzing the performance with the LC- ω PBE functional and def2-TZVPD basis set using the effective tuning parameter (ω_{eff}). The complete data is available in the SI Table S4. For comparison to IP tuning (ω_{IP}), refer to SI Figure S1 and S2.

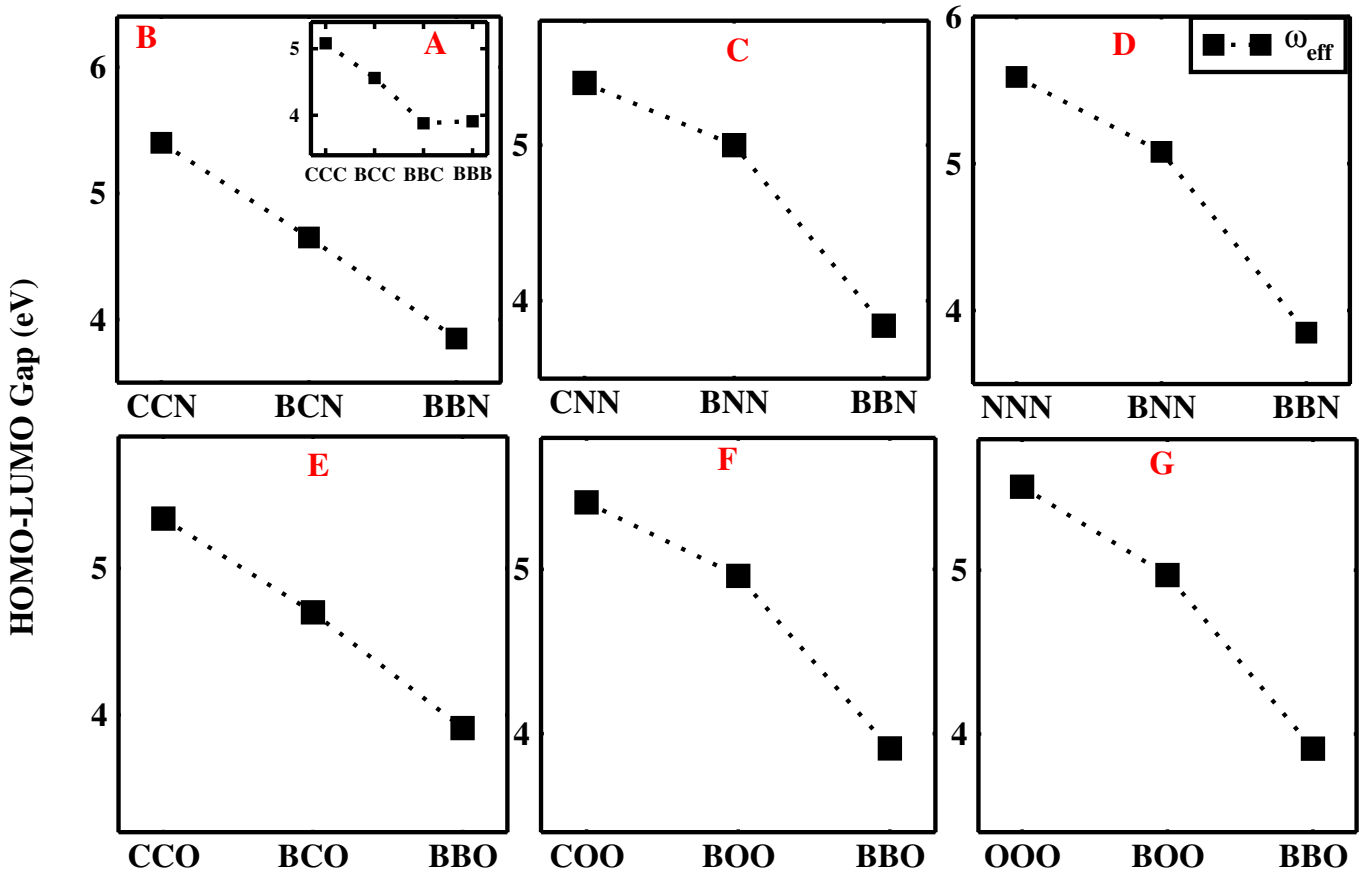


FIG. 3. The HOMO-LUMO gap trends for the doped system, analyzing the performance with the LC- ω PBE functional and def2-TZVPD basis set using the effective tuning parameter (ω_{eff}). The complete data is available in the SI Table S4. For comparison to IP tuning (ω_{IP}), refer to SI Figure S3.

OOC, **COO**, **OCO**, and **BBC**) and mixed-heteroatom (**BNC**, **BCN**, **CBN**, **BCO**, and **CBO**) configurations, giving a total of twelve di-doped systems. The tri-doped set includes both pure (**NNN**, **OOO**, **BBB**) and mixed configurations (**BBN**, **BNN**, **BBO**, **BOO**), providing a total of seven tri-doped systems. Finally, this results in an overall total of 27 doped configurations which are depicted in Fig. 1.

A systematic naming protocol was established where the sequence of letters in the dye's name corresponds to the atom type at each position. For instance, a dye with nitrogen (**N**) at position *a* and carbon (**C**) at positions *b* and *c* is denoted **NCC**, while a dye doped with three nitrogen atoms at positions *a*, *b*, and *c* is named **NNN**. This scheme can be applied for mapping other systems, as illustrated in Figure 1, which provides a clear and consistent label for all variants.

RESULTS AND DISCUSSIONS:

This work investigates a series of newly designed BN-doped (boron and nitrogen), BO-doped (boron and oxy-

gen), and boron-doped π -conjugated organic dyes with a common donor and acceptor. Nitrogen- and oxygen-doped dyes are included from the literature [58], as depicted in Figure 1. These dyes are designed by doping heteroatoms (**N**, **O**, and **B**) at critical positions within the π -conjugated linker or bridge part of the undoped reference dye (**CCC**). The linker connects a carbazole donor to a cyanoacrylic acid acceptor. The whole molecular backbone exhibits an alternating pattern of single and double bonds (known as conjugation). However, one specific carbon atom in each ring of the linker is excluded from this conjugated pathway. Our objective is to dope these critical positions of carbon, labeled *a*, *b*, and *c*, with heteroatoms. This transformation represents an effective strategy to extend the conjugation and enhance delocalization of the electron across the entire system, which helps in facilitating efficient CT in DSSCs. [7, 21, 28]

The primary objective of this work is to deliver reliable predictions of key properties for newly designed heteroatom-doped prototypical dyes, specifically frontier orbital energy levels and singlet-singlet (SS) and singlet-triplet (ST) excitation energies, using an effective tuned DFT/TDDFT protocol across a series of novel organic

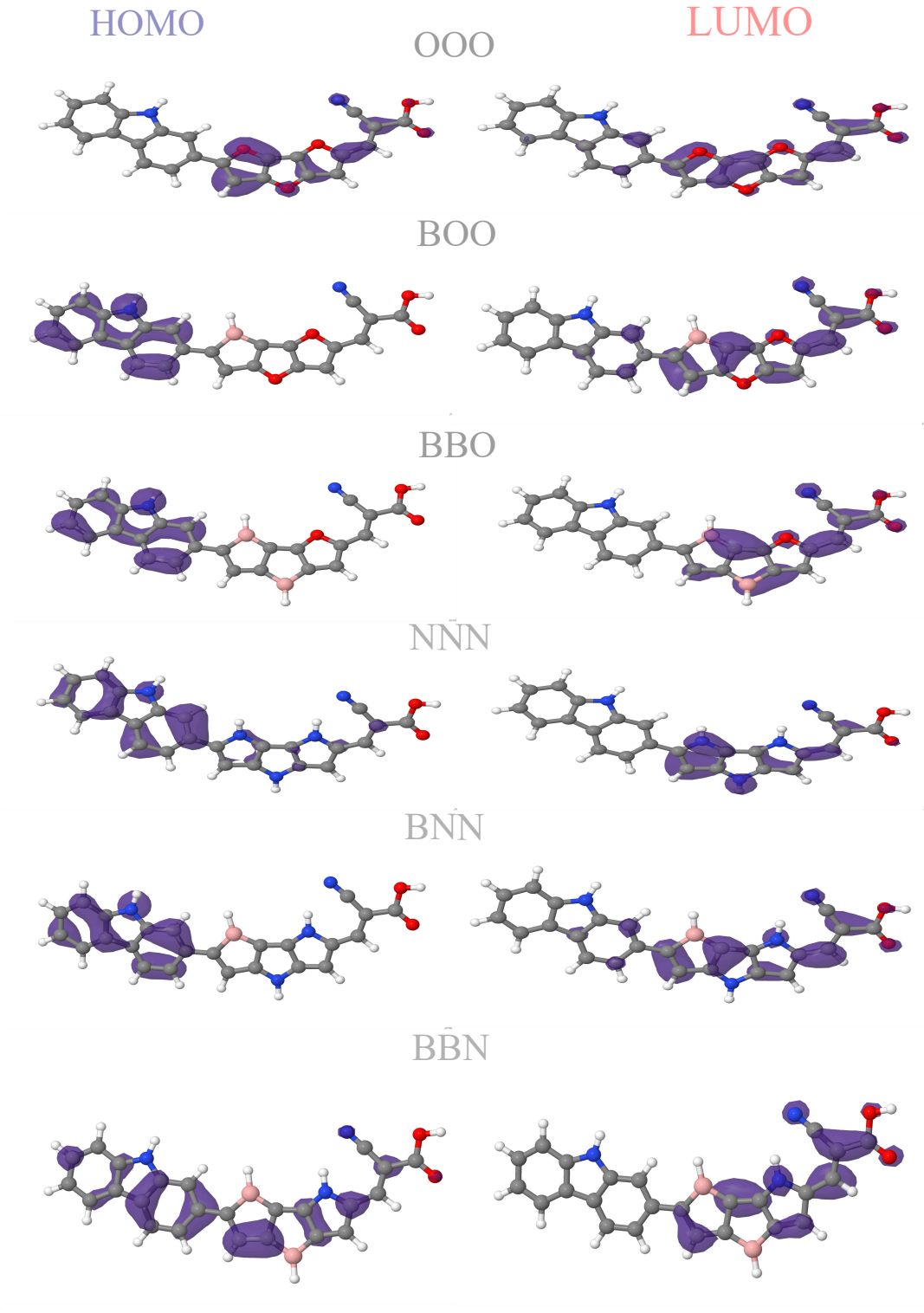


FIG. 4. The spatial distributions of the frontier molecular orbitals (HOMO and LUMO) for O-, B-, and N-doped organic dyes, calculated using the LC- ω_{eff} PBE functional and def2-TZVPD basis set.

dyes.

Initial validation

In order to perform initial validation of this method for doped molecular systems, we applied the ω_{eff} RHS com-

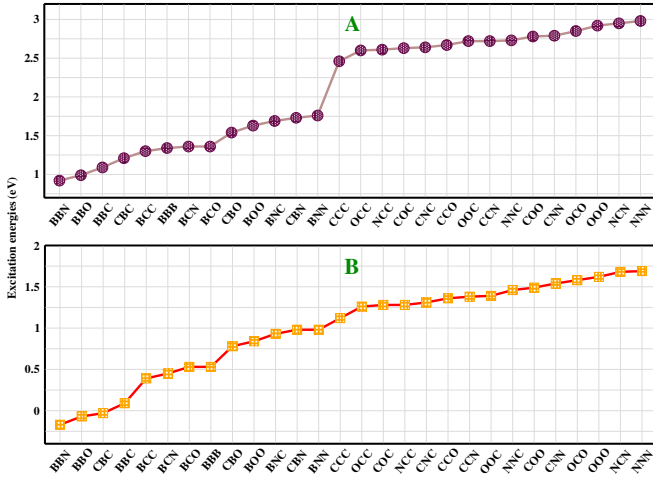


FIG. 5. The singlet-singlet (A) and singlet-triplet (B) excitation energies (eV) of N-, O-, and B-doped organic dyes, analyzing the performance with LC- ω PBE functional and def2-TZVPD basis set using the effective tuning parameter (ω_{eff}). The complete data is available in the SI Table S5. For comparison to IP tuning (ω_{IP}), refer to SI Figure S4.

Molecule	CCSD(T)	LC- ω_{eff} PBE	LC- ω_{IP} PBE	Exp.
BN-1,2 Naph	8.41	8.46	8.36	8.45
BN-1,9 Naph	7.79	7.87	7.73	7.78
BN-9,1-Naph	7.47	7.48	7.38	7.44
BN-9,10-Naph	8.19	8.32	8.29	8.42
MAE (Exp.)	0.08	0.06	0.08	

TABLE I. Vertical ionization potentials in eV calculated using the LC- ω PBE functional with the cc-pVTZ basis set in Q-Chem[22]. The CCSD(T) calculations were carried out using the MOLPRO software package[93]. The geometries of mono-BN-doped naphthalene are from Ref.57, and the UV-visible spectroscopy experimental results are extracted from Ref.50, 57. Mean absolute error (MAE) with respect to experimental values.

putational protocol to four heteroatom-doped organic molecules found in the literature [50, 57], namely BN-1,2-naphthalene, BN-1,9-naphthalene, BN-9,1-naphthalene, and BN-9,10-naphthalene isomers for which experimental vertical IPs (VIPs) data are available. For comparison, we computed the VIPs using the highly accurate CCSD(T) (coupled cluster with single, double, and perturbative triple excitations) method in the cc-pVTZ basis set. These are reported in Table I together with LC- ω PBE result obtained for ω_{eff} and ω_{IP} tuning procedure.

The results indicates that the optimally tuned LC- ω PBE approaches deliver consistently high accuracy for VIPs, reaching near-chemical accuracy (≈ 0.1 eV) at a fraction of the cost of CCSD(T). In particular, the LC- ω_{eff} PBE variant provides the best overall agreement with experiment, yielding the lowest mean absolute error among the tested methods, and showing no large systematic failures across the dataset. The LC- ω PBE accuracy

has been also confirmed in similar context in Ref. 41.

Although the CCSD(T) performs very accurately in this small set, it does not clearly outperform the best-tuned DFT protocol in terms of average deviation from experiment. This underscores an important practical point, namely, for ionization energies in these extended π -systems, well-tuned RSHs can match (or even slightly surpass) CCSD(T) on average, while being far more computationally affordable.

Comparing the two tuning strategies, LC- ω_{eff} PBE is marginally superior to LC- ω_{IP} PBE in overall error statistics. The latter variant shows a slightly larger average deviation, consistent with a mild systematic bias relative to the experiment.

We further note that the parameter ω_{eff} has been extensively validated, demonstrating its ability to reproduce experimental VIPs, to deliver HOMO-LUMO gaps comparable in quality to Green's function methods, and to accurately predict SS excitation energies in organic photovoltaic molecules (see Ref. [76, 77]). Taken together, the results support the claim that effective tuning is a robust and efficient protocol and seems to be an ideal tool for exploring novel organic electronic systems.

HOMO-LUMO Gap

The objective of this work is to precisely control the energy and character of the frontier molecular orbitals (HOMO/LUMO) through targeted doping of the bridge of the core structure of undoped dye (CCC) at specific positions *a*, *b*, and *c* with boron, oxygen, and nitrogen atoms, as shown in Figure 1. The effective-tuning methodology is used to compute the HOMO and LUMO energy levels of all newly designed prototypical organic dyes, which play a crucial role in predicting optoelectronic characteristics and CT in DSSCs. [3, 27] Comparison with IP-tuned results is provided in the Supporting Information (SI) [78](see Figure S1 and S2). Importantly, a strong agreement is observed, as the trends are comparable and the values show minimal deviation between the two tuning procedures. These energy levels are well-aligned in a way that is highly compatible with the key components of the cells, namely the conduction band energy (orange dashed line) and the electrolyte redox potential (cyan dashed line), as depicted in Figure 2A and Figure 2B. For proper device function, the HOMO must be energetically below the redox potential of the electrolyte to enable dye regeneration, while the LUMO must be above the conduction band of the semiconductor to facilitate electron injection. This energetic alignment demonstrates that all dyes possess the characteristics required for a sensitizer and can be considered promising candidates for efficient CT in DSSCs. This also shows that the ω_{eff} RS computational protocol is able to provide relatively fast tools for initial validation

of new DSSC materials.

The sequential substitution of carbon with boron (CCC→BCC→BBC) at positions *a* and *b* of bridge in the core molecular structure of the undoped organic dye (CCC) substantially decreases the HOMO-LUMO gap, reflecting the electron-accepting ability of boron from the adjacent electron donating donor moiety and enhanced π -conjugation, [31, 42] which is crucial for CT. [12, 48] However, this gap increases slightly when the boron is doped at all three positions, namely, *a*, *b*, and *c* to form (BBB). The observed increase in the gap arises due to incorporation of an electron-deficient boron atom at the terminal position *c*, which is located too far from the electron-donating donor, and therefore disrupts the π -electron delocalization that helps to lower the HOMO-LUMO gap, as shown in Figure 3A.

In mono-doped (NCC, CNC, and CCN) and di-doped (NNC, CNN, and NCN) nitrogen-based organic dyes, the HOMO-LUMO gap increases as the position of nitrogen atom moves from (NCC→CNC→CCN) and (NNC→CNN→NCN), respectively, as depicted in Figure 2A. This gap is tunable and can be substantially decreased through the progressive incorporation of boron at positions *a* and *b* (CCN→BCN→BBN, CNN→BNN→BBN) as shown in Figure 3B and 3C, respectively.

In mono-doped (OCC, COC, and CCO) and di-doped (OOC, COO, and OCO) oxygen-based dyes, the HOMO energies are nearly identical. However, the LUMO energies increases slightly when the position of the oxygen atom changes (OCC→COC→CCO) and (OOC→COO→OCO), as shown in Figure 2B. As a result, the observed HOMO-LUMO gap increases across the series. In contrast, this gap decreases significantly with incorporation of boron doping (CCO→BCO→BBO, COO→BOO→BBO) at positions *a* and *b*, as illustrated in Figure 3E and 3F, respectively. The collective information from both approaches demonstrates a consistent trend: mono- and di-doping with heteroatoms (N and O) increases the HOMO-LUMO gap across the series, whereas the sequential introduction of boron atoms significantly decreases it, as shown in Figure S1, S2 and S3 in the SI.

In the tri-doped systems (NNN, OOO, and BBB), the HOMO and LUMO energy levels in the oxygen- and nitrogen-based systems are at different positions. However, their HOMO-LUMO gaps are almost the same. The HOMO-LUMO gap of these two systems is higher than that of the purely boron-based system (BBB). This gap can be systematically reduced by increasing the boron content through atomic substitution at the bridge positions *a* and *b*, as illustrated in Figure 3D and 3G for the sequences (NNN→BNN→BBN) and (OOO→BOO→BBO), respectively. Fig 4 displays the spatial distribution of these frontier orbitals; thus, it can be observed that the reduction in the electronic gap is correlated with a progressive shift of the HOMO

orbital from the bridge and acceptor parts of the organic dye to the donor part. However, the LUMO orbital remains localized over the bridge and acceptor part and is largely intact. This is observed upon sequential incorporation of boron at positions *a* and *b* in both the NNN and OOO parent systems, forming the BNN/BBN and BOO/BBO systems, respectively. The smallest gap among all variants is observed in the BBN dye, which is doped with two boron (B) atoms at positions *a* and *b* and one nitrogen (N) atom at position *c* on the bridge.

Singlet-Singlet and Singlet-Triplet Excitation Energies

The general trends of SS and ST excitation energies for the series of doped dyes are presented systematically in increasing order in Figure 5A and 5B, respectively. These excitation energies are obtained using both effective and IP-tuning methodologies (see Figure S4 in SI file). Both tuning procedures predict the same overall behavior, differing only slightly in a few isolated cases, which supports our analysis. The undoped organic dye (CCC) is used as the reference for interpreting the results. Overall, the data reveal two distinct, opposing trends controlled by the electronic character of the heteroatom dopants—specifically, whether the dopant acts as an electron donor or acceptor. Incorporation of electron-rich, lone-pair-bearing heteroatoms such as nitrogen and oxygen markedly increases the excitation energies relative to CCC. This increase is larger for nitrogen-doped systems than for their oxygen-doped counterparts. The corresponding blue shift is consistent across mono-, di-, and tri-doped N- and O-containing dyes. Moreover, the excitation energy increases systematically with dopant count (N or O): tri-doped dyes exhibit higher energies than di-doped dyes, which in turn exceed those of mono-doped dyes.

In contrast, the incorporation of the electron-deficient boron (B) atom is a highly effective strategy for tuning the optical properties, as it systematically and significantly reduces this excitation energy, leading to a pronounced red-shift. This effect follows a clear concentration dependence across all doping levels, as demonstrated by the progressive decrease in SS and ST excitation energies along sequences in mono-doped (CCN→BCN→BBN, CCO→BCO→BBO), di-doped (CNN→BNN→BBN, COO→BOO→BBO), and tri-doped (NNN→BNN→BBN, OOO→BOO→BBO) systems, as illustrated in Figure 5. For ST excitation we observe negative excitation energies for BBN, BBO and CBC systems. This reveals their diradical nature and demonstrates that the triplet state is unstable, a finding consistent with earlier studies for TDDFT[62, 72], and also for WFT and multireference methods[24, 69, 87].

Among all newly designed dyes, the BBN dye exhibits the lowest SS and ST excitation energies.

CONCLUSION

CT dye discovery for DSSCs requires exploring a large chemical space while preserving predictive accuracy for frontier-orbital alignment and low-lying excited states. In practice, this creates a central bottleneck: high-level WFT methods are often very expensive for systematic screening, while conventional tuning of RSH functionals (e.g., IP tuning) adds substantial overhead that limits throughput and dataset scale. Addressing this challenge, we analyzed and deployed a novel single-shot effective-tuning protocol, ω_{eff} , as a simple and cost-effective alternative to IP tuning for determining the optimal RS parameter in LR corrected hybrid functionals, while maintaining accuracy close to WFT benchmarks.

A key outcome of this work is that the availability of a reliable, low-cost tuning strategy enables *effective screening* and, therefore, rational *design* of new CT candidates. Specifically, the validated protocol ω_{eff} allowed us to systematically construct and characterize an organized benchmark/library set of 27 mono-, di-, and tri-doped organic dyes based on the D- π -A model consisting of a common carbazole donor and cyanoacrylic acid acceptor, with targeted substitutions at three critical bridge sites (*a*, *b*, and *c*) using N, O, and B dopants. This dataset provides a consistent platform for extracting clear structure property relationships and guiding future candidate selection in a way that would be significantly more difficult with costlier tuning procedures or WFT-based screening.

Across this doped dye library, we show that electronic and optical properties can be strongly tuned through strategic heteroatom doping at the bridge positions. Doping with electron-rich nitrogen or oxygen generally increases the HOMO-LUMO gap as well as the SS and ST excitation energies, with a markedly stronger effect for nitrogen than for oxygen. Moreover, for N- and O-containing series, the excitation energies increase progressively with the number of dopants, following the order: mono-doped < di-doped < tri-doped dyes, consistent with systematic blue shifts. In contrast, the sequential incorporation of electron-deficient boron at these sites substantially reduces the HOMO-LUMO gap and lowers both SS and ST excitation energies, producing pronounced red shifts. Fundamentally, these opposing trends stem from the donor versus acceptor character of the dopants and their impact on π -electron delocalization and frontier orbital localization within the donor-bridge-acceptor framework. Collectively, these results establish boron incorporation as a powerful strategy for engineering sensitizers with reduced gaps and lower excitation energies, which are key ingredients for efficient light har-

vesting and charge separation in DSSCs.

More broadly, this work demonstrates the expanded utility of LR-corrected hybrid functionals for materials design and highlights ω_{eff} as a computationally efficient and accessible pathway to accurate predictions relevant to CT. By lowering the cost barrier to systematic exploration, the effective-tuning protocol enables the creation of curated benchmark libraries and supports the rapid screening and rational design of novel donor-acceptor architectures. Future work will extend this framework to more device-realistic modeling, including solvent and interfacial effects, explicit dye-TiO₂ binding motifs, and additional CT descriptors, to further connect molecular-level screening to experimentally measurable DSSC performance metrics.

ACKNOWLEDGEMENTS

S.Ś. acknowledges the financial support from the National Science Centre, Poland (grant no. 2021/42/E/ST4/00096). R. D. P. gratefully acknowledges financial support from the Polish National Agency for Academic Exchange (NAWA). R. D. P. and P. T. acknowledge financial support from the PRELUDIUM BIS research grant from the National Science Centre, Poland (Grant No. 2023/50/O/ST4/00353). The computational work for this study was performed during a three-month research visit at the National Institute of Science Education and Research (NISER) in Bhubaneswar, India. The authors gratefully acknowledge the use of the HPC cluster Kalinga, located in the School of Physical Sciences at NISER.

DATA AVAILABILITY

The data that support the findings are published within this study.

CONFLICTS OF INTEREST

There are no conflicts to declare.

* aditisinh4812@doktorant.umk.pl, aditisinh4812@gmail.com
 † rampandey@doktorant.umk.pl, pandey123iitian@gmail.com
 ‡ szsmiga@fizyka.umk.pl

[1] Study of photosensitizer dyes for high-performance dye-sensitized solar cells application: A computational investigation. *Chem. Phys. Impact.*, 9:100719, 2024.
 [2] Wajid Ali, Anjali Dahiya, Ramdhari Pandey, Tipu Alam, and Bhisma K. Patel. Microwave-assisted cascade strategy for the synthesis of indolo[2,3-b]quinolines from 2-

(phenylethynyl)anilines and aryl isothiocyanates. *J. Org. Chem.*, 82(4):2089–2096, 2017.

[3] William Ojoniko Anthony, Muhammed Kabir Abubakar, Kehinde Gabriel Obiyenwa, Ibrahim Olasegun Abdulsalami, Olalekan Wasiu Salaw, and Banjo Semire. Computational design of phenoxazine and phenothiazine dye sensitizers with improved charge separation for application in dsscs: a dft study. *Discov. chem.*, 2(1):1–26, 2025.

[4] Ahmed Azaid, Marzouk Raftani, Marwa Alaqrarbeh, Rchid Kacimi, Tayeb Abram, Youness Khaddam, Diaa Nebbach, Abdelouahid Sbai, Tahar Lakhli, and Mohammed Bouachrine. New organic dye-sensitized solar cells based on the d-a- π -a structure for efficient dsscs: Dft/td-dft investigations. *RSC Adv.*, 12:30626–30638, 2022.

[5] Han-Seok Bae, Dae-Hwan Ahn, and Jong-Won Song. Why does the optimal tuning method of the range separation parameter of a long-range corrected density functional fail in intramolecular charge transfer excitation calculations? *Molecules*, 29(18), 2024. URL: <https://www.mdpi.com/1420-3049/29/18/4423>, doi:10.3390/molecules29184423.

[6] Axel D Becke. Density-functional exchange-energy approximation with correct asymptotic behavior. *Phys. rev. A*, 38(6):3098, 1988.

[7] Si Mohamed Bouzzine, Alioui Abdelaaziz, Mohamed Hamidi, Fatimah A. M. Al-Zahrani, Mohie E. M. Zayed, and Reda M. El-Shishtawy. The impact of tpa auxiliary donor and the π -linkers on the performance of newly designed dye-sensitized solar cells: Computational investigation. *Materials*, 16(4), 2023.

[8] Ute B. Cappel, Martin H. Karlsson, Neil G. Pschirer, Felix Eickemeyer, Jan Schöneboom, Peter Erk, Gerrit Boschloo, and Anders Hagfeldt. A broadly absorbing perylene dye for solid-state dye-sensitized solar cells. *J. Phys. Chem. C*, 113(33):14595–14597, 2009.

[9] Marcos Casanova-Páez and Lars Goerigk. Assessing the tamm-dancoff approximation, singlet-singlet, and singlet-triplet excitations with the latest long-range corrected double-hybrid density functionals. *J. Chem. Phys.*, 153(6):064106, 08 2020.

[10] M. E. Casida. *Recent Advances in Density Functional Methods, Part I*. Word Scientific, 1995.

[11] MARK E. CASIDA. *Time-Dependent Density Functional Response Theory for Molecules*, pages 155–192.

[12] Yanke Che, Aniket Datar, Xiaomei Yang, Tammene Naddo, Jincai Zhao, and Ling Zang. Enhancing one-dimensional charge transport through intermolecular π -electron delocalization: Conductivity improvement for organic nanobelts. *J. Am. Chem. Soc.*, 129(20):6354–6355, 2007.

[13] Vacestlav Coropceanu, Jérôme Cornil, Demetrio A. da Silva Filho, Yoann Olivier, Robert Silbey, and Jean-Luc Brédas. Charge transport in organic semiconductors. *Chemical Reviews*, 107(4):926–952, 2007.

[14] J. CÃlsar Cruz, Ernest Opoku, Szymon Smiga, Ireneusz Grabowski, Joseph Vincent Ortiz, and So Hirata. Performance of the spin-component-scaled methods for energy bands. *Molecular Physics*, 123(19-20):e2504545, 2025. arXiv:<https://doi.org/10.1080/00268976.2025.2504545>, doi:10.1080/00268976.2025.2504545.

[15] Stefano Curtarolo, Gus L. W. Hart, Marco Buongiorno Nardelli, Natalio Mingo, Stefano Sanvito, and Ohad Levy. The high-throughput highway to computational materials design. *Nat. Mater.*, 12(3):191–201, mar 2013.

[16] Tomás Delgado-Montiel, Jesús Baldenebro-López, Rody Soto-Rojo, and Daniel Grossman-Mitnik. Theoretical study of the effect of π -bridge on optical and electronic properties of carbazole-based sensitizers for dsscs. *Molecules*, 25(16):3670, 2020.

[17] Andreas Dreuw and Martin Head-Gordon. Single-reference ab initio methods for the calculation of excited states of large molecules. *Chemical Reviews*, 105(11):4009–4037, 2005. PMID: 16277369. doi:10.1021/cr0505627.

[18] Harkishan Dua, Debolina Paul, and Utpal Sarkar. A study on indolo [3, 2, 1- jk] carbazole donor-based dye-sensitized solar cells and effects from addition of auxiliary donors. *Phys. Chem. Chem. Phys.*, 27(5):2720–2731, 2025.

[19] Jr. Dunning, Thom H. Gaussian basis sets for use in correlated molecular calculations. I. The atoms boron through neon and hydrogen. *J. Chem. Phys.*, 90(2):1007–1023, 01 1989.

[20] Naresh Duvva, Ravi Kumar Kanaparthi, Jaipal Kandhadi, Gabriele Marotta, Paolo Salvatori, Filippo De Angelis, and Lingamallu Giribabu. Carbazole-based sensitizers for potential application to dye sensitized solar cells. *J. Chem. Sci.*, 127(3):383–394, 2015.

[21] Mohamed R Elmorsy, Samar M Mohammed, Basant A Mohamed, Ahmed H Moustafa, and Safa A Badawy. High-efficiency tandem dsscs based on tailored naphthalene sensitizers for indoor dssc efficiency above 25%. *Sci. Rep.*, 2025.

[22] Evgeny Epifanovsky and et al. Gilbert. Software for the frontiers of quantum chemistry: An overview of developments in the q-chem 5 package. *J. Chem. Phys.*, 155(8):084801, 08 2021.

[23] Edson Evangelista, Iva S. de Jesus, Fernanda P. Pauli, Acácio S. de Souza, Amanda de A. Borges, Maria Vitória S. F. Gomes, Vitor F. Ferreira, Fernando de C. da Silva, Mauricio A. Melo, and Luana da S. M. Forezi. Recent advances in the application of coumarins as photosensitizers for the construction of a dye-sensitized solar cell. *ACS Omega*, 10(14):13726–13748, 2025.

[24] Soumen Ghosh and Kalishankar Bhattacharyya. Origin of the failure of density functional theories in predicting inverted singlet-triplet gaps. *J. Phys. Chem. A*, 126(8):1378–1385, 2022.

[25] Marco Giordano, Francesca Cardano, Claudia Barolo, Guido Viscardi, and Andrea Fin. Perylene-based dyes in dye-sensitized solar cells: Structural development and synthetic strategies. *Adv. Funct. Mater.*, 35(1):2411230, 2025.

[26] A. Görling. Time-dependent Kohn–Sham formalism. *Phys. Rev. A*, 55:2630, 1997.

[27] Pramesh Gunawardhana, Yashas Balasooriya, Murthi S. Kandananpitie, Yuan-Fong Chou Chau, Muhammad Raziq Rahimi Kooh, and Roshan Thotagamuge. Optoelectronic characterization of natural dyes in the quest for enhanced performance in dye-sensitized solar cells: A density functional theory study. *Appl. Sci.*, 14(1), 2024.

[28] Shuang Guo, Yeonju Park, Eungyeong Park, Sila Jin, Lei Chen, and Young Mee Jung. Molecular-orbital delocalization enhances charge transfer in π -conjugated organic semiconductors. *Angew. Chem. Int. Ed.*, 62(34):e202306709, 2023.

[29] Daniel P Hagberg, Tannia Marinado, Karl Martin Karlsson, Kazuteru Nonomura, Peng Qin, Gerrit Boschloo, Tore Brinck, Anders Hagfeldt, and Licheng Sun. Tuning the homo and lumo energy levels of organic chromophores for dye sensitized solar cells. *J. Org. Chem.*, 72(25):9550–9556, 2007.

[30] Robert M. Hanson. *Jmol* – a paradigm shift in crystallographic visualization. *J. Appl. Crystallogr.*, 43(5 Part 2):1250–1260, Oct 2010.

[31] Daniel Hashemi, Xiao Ma, Ramin Ansari, Jinsang Kim, and John Kieffer. Design principles for the energy level tuning in donor/acceptor conjugated polymers. *Phys. Chem. Chem. Phys.*, 21(2):789–799, 2019.

[32] So Hirata and Martin Head-Gordon. Time-dependent density functional theory within the tamm-dancoff approximation. *Chem. Phys. Lett.*, 314(3):291–299, 1999.

[33] Denis Jacquemin, Eric A. Perp  te, Gustavo E. Scuseria, Ilaria Ciofini, and Carlo Adamo. Td-dft performance for the visible absorption spectra of organic dyes: Conventional versus long-range hybrids. *J. Chem. Theory Comput.*, 4(1):123–135, 2008.

[34] Denis Jacquemin, Val  rie Wathelet, Eric A. Perp  te, and Carlo Adamo. Extensive td-dft benchmark: Singlet-excited states of organic molecules. *J. Chem. Theory Comput.*, 5(9):2420–2435, 2009.

[35] R Kacimi, M Raftani, T Abram, A Azaid, H Ziyat, L Bejjit, MN Bennani, and M Bouachrine. Theoretical design of d-  -a system new dyes candidate for dssc application. *Helion*, 7(6), 2021.

[36] Rachid Kacimi, Mohamed Bourass, Thierry Toupance, Nuha Wazzan, Mourad Chemek, Aziz El Alamy, Lahcen Bejjit, Kamel Alimi, and Mohammed Bouachrine. Computational design of new organic (d-  -a) dyes based on benzothiadiazole for photovoltaic applications, especially dye-sensitized solar cells. *Res. Chem. Intermed.*, 46(6), 2020.

[37] Prashant V Kamat. Manipulation of charge transfer across semiconductor interface. a criterion that cannot be ignored in photocatalyst design. *J. Phys. Chem. Lett.*, 3(5):663–672, 2012.

[38] Ganapathi Rao Kandregula, Sudip Mandal, Chinmaya Mirle, and Kothandaraman Ramanujam. A computational approach on engineering short spacer for carbazole-based dyes for dye-sensitized solar cells. *J. Photochem. Photobiol. A: Chem.*, 419:113447, 2021.

[39] Markus D. K  rk  s, Oscar Verho, Eric V. Johnston, and Bj  rn   kermark. Artificial photosynthesis: Molecular systems for catalytic water oxidation. *Chem. Rev.*, 114(24):11863–12001, 2014.

[40] Rick A. Kendall, Jr. Dunning, Thom H., and Robert J. Harrison. Electron affinities of the first-row atoms revisited. systematic basis sets and wave functions. *J. Chem. Phys.*, 96(9):6796–6806, 05 1992.

[41] Hyunsik Kim, Ajith Perera, Rodrigo A. Mendes, and Rodney J. Bartlett. Benchmarking ionization potentials and electron affinities of potential photovoltaic molecules using dft/qtp functionals and eom-cc. *The Journal of Chemical Physics*, 163(17):174703, 11 2025. [arXiv:https://pubs.aip.org/aip/jcp/article-pdf/doi/10.1063/5.0293131](https://pubs.aip.org/aip/jcp/article-pdf/doi/10.1063/5.0293131)

[42] Naveen Kosar, Saba Kanwal, Malai Haniti S. A. Hamid, Khurshid Ayub, Mazhar Amjad Gilani, Muhammad Imran, Muhammad Arshad, Mohammed A. Alkhalfah, Nadeem S. Sheikh, and Tariq Mahmood. Role of de localization, asymmetric distribution of π -electrons and elongated conjugation system for enhancement of nlo response of open form of spiropyran-based thermochromes. *Molecules*, 28(17), 2023.

[43] Bal  zs Kozma, Attila Tajti, Baptiste Demoulin, R  bert Izs  k, Marcel Nooijen, and P  ter G. Szalay. A new benchmark set for excitation energy of charge transfer states: Systematic investigation of coupled cluster type methods. *J. Chem. Theory Comput.*, 16(7):4213–4225, 2020.

[44] Leeor Kronik, Tamar Stein, Sivan Refaeli-Abramson, and Roi Baer. Excitation gaps of finite-sized systems from optimally tuned range-separated hybrid functionals. *J. Chem. Theory Comput.*, 8(5):1515–1531, 2012.

[45] Vignesh Balaji Kumar, Szymon   miga, and Ireneusz Grabowski. A critical evaluation of the hybrid ks dft functionals based on the ks exchange-correlation potentials. *J. Phys. Chem. Lett.*, 15(40):10219–10229, 2024.

[46] Malak Lazrak, Hamid Toufik, Si Mohamed Bouzzine, and Fatima Lamchouri. Bridge effect on the charge transfer and optoelectronic properties of triphenylamine-based organic dye sensitized solar cells: theoretical approach. *Res. Chem. Intermed.*, 46(8):3961–3Res. Chem. Intermed.978, 2020.

[47] Jaehee Lee and Woon Ju Song. Photocatalytic c-o coupling enzymes that operate via intramolecular electron transfer. *J. Am. Chem. Soc.*, 145(9):5211–5221, 2023.

[48] Yujie Liang, Chi Cao, Lei Zeng, Haonan Wang, and Yabin Jiang. Simultaneously improving the delocalization of π electrons and directional transfer of charge carriers in carbon nitride for superior photocatalytic hydrogen evolution. *J. Mater. Chem. A*, 12:26096–26102, 2024.

[49] Bo Liu, Bao Wang, Ran Wang, Lin Gao, Suhong Huo, Qingbin Liu, Xiaoyan Li, and Weihong Zhu. Influence of conjugated π -linker in d-d-  -a indoline dyes: towards long-term stable and efficient dye-sensitized solar cells with high photovoltage. *J. Mater. Chem. A*, 2(3):804–812, 2014.

[50] Zhiqiang Liu, Jacob S. A. Ishibashi, Clovis Darrigan, Alain Dargelos, Anna Chrostowska, Bo Li, Monica Vasiliu, David A. Dixon, and Shih-Yuan Liu. The least stable isomer of bn naphthalene: Toward predictive trends for the optoelectronic properties of bn acenes. *J. Am. Chem. Soc.*, 139(17):6082–6085, 2017.

[51] R. J. Magyar and S. Tretiak. Dependence of spurious charge-transfer excited states on orbital exchange in tddft: Large molecules and clusters. *J. Chem. Theory Comput.*, 3(3):976–987, 2007.

[52] Aniket Mandal and John M. Herbert. Simplified tuning of long-range corrected time-dependent density functional theory. *J. Phys. Chem. Lett.*, 16(10):2672–2680, 2025.

[53] Amaresh Mishra, Markus KR Fischer, and Peter B  uerle. Metal-free organic dyes for dye-sensitized solar cells: From structure: Property relationships to design rules. *Angew. Chem. Int. Ed.*, 48(14):2474–2499, 2009.

[54] Ramsha Munir, Ameer Fawad Zahoor, Muhammad Naveed Anjum, Usman Nazeer, Atta Ul Haq, Asim Mansha, Aijaz Rasool Chaudhry, and Ahmad Irfan. Synthesis of organic dyes based on spirobifluorene (SOF) and their use as photosensitizers in dye-sensitized solar cells (dssc): A review. *Top. Curr. Chem.*, 383(1):5, 2024.

[55] F. Neese. Software update: the orca program system, version 5.0. *WIREs Comput. Molec. Sci.*, 12(1):e1606, 2022.

[56] Giovanni Onida, Lucia Reining, and Angel Rubio. Electronic excitations: density-functional versus many-body green's-function approaches. *Rev. Mod. Phys.*, 74:601–659, Jun 2002. URL: <https://link.aps.org/doi/10.1103/RevModPhys.74.601>, doi:10.1103/RevModPhys.74.601.

[57] Ram Dhari Pandey, Matheus Morato F. de Moraes, Katharina Boguslawski, and Paweł Tecmer. Frozen-pair-type pccd-based methods and their double ionization variants to predict properties of prototypical bn-doped light emitters. *J. Chem. Theory Comput.*, 21(10):5049–5061, 2025.

[58] Ram Dhari Pandey, Marta Galyńska, Katharina Boguslawski, and Paweł Tecmer. Tuning domain-based charge transfer in organic dyes: Impact of heteroatom doping on the π -linker of carbazole-based systems. *J. Phys. Chem. A*, 0(0):null, 0. PMID: 41466577, doi:10.1021/acs.jpca.5c07039.

[59] Kenley M. Pelzer, Álvaro Vázquez-Mayagoitia, Laura E. Ratcliff, Sergei Tretiak, Raymond A. Bair, Stephen K. Gray, Troy Van Voorhis, Ross E. Larsen, and Seth B. Darling. Molecular dynamics and charge transport in organic semiconductors: a classical approach to modeling electron transfer. *Chemical Science*, 8:2597–2609, 2017.

[60] John P Perdew. Density-functional approximation for the correlation energy of the inhomogeneous electron gas. *Phys. rev. B*, 33(12):8822, 1986.

[61] M. Petschow, E. Peise, and P. Bientinesi. High-performance solvers for dense hermitian eigenproblems. *SIAM J. Sci. Comput.*, 35(1):C1–C22, 2013.

[62] Felix Plasser. On the meaning of de-excitations in time-dependent density functional theory computations. *J. Comput. Chem.*, 46(8):e70072, 2025.

[63] Danny Porath, Alexey Bezryadin, Simon de Vries, and Cees Dekker. Direct measurement of electrical transport through dna molecules. *Nature*, 403(6770):635–638, 2000.

[64] Tonatiuh Rangel, Samia M. Hamed, Fabien Bruneval, and Jeffrey B. Neaton. An assessment of low-lying excitation energies and triplet instabilities of organic molecules with an ab initio bethe-salpeter equation approach and the tamm-danoff approximation. *J. Chem. Phys.*, 146(19):194108, 05 2017.

[65] Sivan Refaelly-Abramson, Sahar Sharifzadeh, Niranjan Govind, Jochen Autschbach, Jeffrey B. Neaton, Roi Baer, and Leeor Kronik. Quasiparticle spectra from a nonempirical optimally tuned range-separated hybrid density functional. *Phys. Rev. Lett.*, 109:226405, Nov 2012.

[66] Mary A. Rohrdanz and John M. Herbert. Simultaneous benchmarking of ground- and excited-state properties with long-range-corrected density functional theory. *The Journal of Chemical Physics*, 129(3):034107, 07 2008.

[67] Hossein Roohi and Nafiseh Mohtamadifar. The role of the donor group and electron-accepting substitutions inserted in π -linkers in tuning the optoelectronic properties of d– π –a dye-sensitized solar cells: a dft/tddft study. *RSC adv.*, 12(18):11557–11573, 2022.

[68] Mostafa Saad Ebied, Mahmoud Dongol, Medhat Ibrahim, Mohammed Nassary, Sahar Elnobi, and Amr Attia Abuelwafa. Effect of carboxylic acid and cyanoacrylic acid as anchoring groups on coumarin 6 dye for dye-sensitized solar cells: Dft and td-dft study. *Struct. Chem.*, 33(6):1921–1933, 2022.

[69] J. Sanz-Rodrigo, G. Ricci, Y. Olivier, and J. C. Sancho-García. Negative singlet-triplet excitation energy gap in triangle-shaped molecular emitters for efficient triplet harvesting. *J. Phys. Chem. A*, 125(2):513–522, 2021.

[70] João Sarrato, Ana Lucia Pinto, Gabriela Malta, Eva G. Röck, João Pina, João Carlos Lima, A. Jorge Parola, and Paula S. Branco. New 3-ethynylaryl coumarin-based dyes for dssc applications: Synthesis, spectroscopic properties, and theoretical calculations. *Molecules*, 26(10), 2021.

[71] Marko Schreiber, Mario R. Silva-Junior, Stephan P. A. Sauer, and Walter Thiel. Benchmarks for electronically excited states: Caspt2, cc2, ccscd, and cc3. *J. Chem. Phys.*, 128(13):134110, 04 2008. arXiv:<https://pubs.aip.org/aip/jcp/article-pdf/doi/10.1063/1.2889385>.

[72] John S. Sears, Thomas Koerzdoerfer, Cai-Rong Zhang, and Jean-Luc Brédas. Communication: Orbital instabilities and triplet states from time-dependent density functional theory and long-range corrected functionals. *J. Chem. Phys.*, 135(15):151103, 10 2011.

[73] G. D. Sharma, J. A. Mikroyannidis, M. S. Roy, K. R. Justin Thomas, R. J. Ball, and Rajnish Kurchania. Dithienylthienothiadiazole-based organic dye containing two cyanoacrylic acid anchoring units for dye-sensitized solar cells. *RSC Adv.*, 2:11457–11464, 2012.

[74] Aditi Singh. Molecular geometries of doped organic dye systems, 2025. URL: <https://github.com/aditisinha4812/Doped-systems>.

[75] Aditi Singh. Tuned range separated made simple, 2025. URL: https://github.com/aditisinha4812/tuned_range_separated_made_simple.

[76] Aditi Singh, Subrata Jana, Lucian A. Constantin, Fabio Della Sala, Prasanjit Samal, and Szymon Śmiga. Simplified, physically motivated, and broadly applicable range-separation tuning. *J. Phys. Chem. Lett.*, 16(32):8198–8208, 2025.

[77] Aditi Singh, Subrata Jana, and Szymon Śmiga. Effective range-separated starting points for single-shot g_{0w0} for molecules and clusters. Submitted, 2026.

[78] Aditi Singh, Ram Dhari Pandey, Subrata Jana, Prasanjit Samal, Paweł Tecmer, and Szymon Śmiga. Supplementary material: A simplified approach for modulating frontier orbitals of prototypical organic dyes for efficient dye-sensitized solar cells. Supplementary Material, January 2026. Additional data, and extended results.

[79] Spiros S Skourtis, David H Waldeck, and David N Beratan. Fluctuations in biological and bioinspired electron-transfer reactions. *Annu. Rev. Phys. Chem.*, 61(1):461–485, 2010.

[80] Roberto Sole, Marco Bortoluzzi, Anke Spannenberg, Sergey Tin, Valentina Beghetto, and Johannes G. de Vries. Synthesis, characterization and catalytic activity of novel ruthenium complexes bearing nnn click based ligands. *Dalton Trans.*, 48:13580–13588, 2019.

[81] Tamar Stein, Leeor Kronik, and Roi Baer. Reliable prediction of charge transfer excitations in molecular complexes using time-dependent density functional theory. *J. Am. Chem. Soc.*, 131(8):2818–2820, 2009.

[82] Pit Steinbach and Christoph Bannwarth. Combining low-cost electronic structure theory and low-cost parallel computing architecture. *Phys. Chem. Chem. Phys.*, 26:16567–16578, 2024.

[83] Qiming Sun, Xing Zhang, Samragni Banerjee, and Peng Bao. Recent developments in the pyscf program package. *J. Chem. Phys.*, 153(2):024109, 07 2020.

[84] A. Szabo and N.S. Ostlund. *Modern Quantum Chemistry: Introduction to Advanced Electronic Structure Theory*. Dover Books on Chemistry. Dover Publications, 1996.

[85] Lena Szczuczko, Marta Gałyńska, Maximilian H. Kriebel, Paweł Tecmer, and Katharina Boguslawski. Domain-based charge-transfer decomposition and its application to explore the charge-transfer character in prototypical dyes. *J. Chem. Theory Comput.*, 21(9):4506–4519, 2025.

[86] Yunyu Tang, Yueqiang Wang, Xin Li, Hans Ågren, Wei-Hong Zhu, and Yongshu Xie. Porphyrins containing a triphenylamine donor and up to eight alkoxy chains for dye-sensitized solar cells: a high efficiency of 10.9%. *ACS Appl. Mater. Interfaces*, 7(50):27976–27985, 2015.

[87] Lucie Tučková, Michal Straka, Rashid R. Valiev, and Dage Sundholm. On the origin of the inverted singlet-triplet gap of the 5th generation light-emitting molecules. *Phys. Chem. Chem. Phys.*, 24(31):18713–18721, 2022.

[88] Talapunur Vikramaditya, Jeng-Da Chai, and Shiang-Tai Lin. Impact of non-empirically tuning the range-separation parameter of long-range corrected hybrid functionals on ionization potentials, electron affinities, and fundamental gaps. *Journal of Computational Chemistry*, 39(28):2378–2384, 2018.

[89] Oleg A. Vydrov and Gustavo E. Scuseria. Assessment of a long-range corrected hybrid functional. *J. Chem. Phys.*, 125(23):234109, 12 2006.

[90] Youfu Wang, Luhua Dong, Zhiwei Zheng, Xing Li, Rulin Xiong, Jianli Hua, and Aiguo Hu. Enediyne as π linker in d- π -a dyes for dye-sensitized solar cells. *RSC Adv.*, 6(15):12124–12130, 2016.

[91] Z-S Wang, Yan Cui, Kohjiro Hara, Yasufumi Danoh, Chiaki Kasada, and Akira Shinpo. A high-light-harvesting-efficiency coumarin dye for stable dye-sensitized solar cells. *J. Adv. Mater.*, 19(8):1138–1141, 2007.

[92] Michael R. Wasielewski. Energy, charge, and spin transport in molecules and self-assembled nanostructures inspired by photosynthesis. *J. Org. Chem.*, 71(14):5051–5066, 2006.

[93] Hans-Joachim Werner, Peter J. Knowles, Frederick R. Manby, Joshua A. Black, Klaus Doll, Andreas Heßelmann, Daniel Kats, Andreas Köhn, Tatiana Korona, David A. Kreplin, Qianli Ma, III Miller, Thomas F., Alexander Mitrushchenkov, Kirk A. Peterson, Iakov Polyak, Guntram Rauhut, and Marat Sibaev. The molpro quantum chemistry package. *J. Chem. Phys.*, 152(14):144107, 04 2020.

[94] Wei Xu, Bo Peng, Jun Chen, Mao Liang, and Fengshi Cai. New triphenylamine-based dyes for dye-sensitized solar cells. *J. Phys. Chem. C*, 112(3):874–880, 2008.

[95] Takeshi Yanai, David P Tew, and Nicholas C Handy. A new hybrid exchange-correlation functional using the coulomb-attenuating method (cam-b3lyp). *Chem. Phys. Lett.*, 393(1):51–57, 2004.

[96] Xichuan Yang, Jianghua Zhao, Lei Wang, Jie Tian, and Licheng Sun. Phenothiazine derivatives-based d- π -a and d-a- π -a organic dyes for dye-sensitized solar cells. *RSC Adv.*, 4(46):24377–24383, 2014.

[97] Cai-Rong Zhang, Li Liu, Jian-Wu Zhe, Neng-Zhi Jin, Yao Ma, Li-Hua Yuan, Mei-Lin Zhang, You-Zhi Wu, Zi-Jiang Liu, and Hong-Shan Chen. The role of the conjugate bridge in electronic structures and related properties of tetrahydroquinoline for dye sensitized solar cells. *Int. J. Mol. Sci.*, 14(3):5461–5481, 2013.

[98] Lei Zhang and Jacqueline M. Cole. Anchoring groups for dye-sensitized solar cells. *ACS Appl. Mater. Interfaces*, 7(6):3427–3455, 2015.